

Identification and astrometry of variables in M3

by

Gáspár Á. Bakos^{*†}, József M. Benkő and Johanna Jurcsik
Konkoly Observatory, P. O. Box 67, H-1525 Budapest, Hungary

October 30, 2018

Abstract

We present identification and astrometry of all previously known or suspected variables along with the discovery of six new variables in the globular cluster M3. The number of the catalogized variables increased to 274 by including all the confirmed, previously known variables and the new discoveries. The precise and homogeneous astrometry, as well as the clarification of misapprehensions in the preceding identifications are done by using overlapping fields from a wide-field Schmidt-camera, a 1m RCC telescope, and HST archive observations from the center of the cluster. The astrometric positions can serve as a direct input to any photometry which needs the accurate centers of the variables.

Key words: *stars: variables: general*

1 Introduction

Starting with the discovery of a W Vir star in M3 [Pickering(1889)], which was the first pulsating variable to be observed in any globular cluster, M3 deserved the reputation of being the richest globular cluster in variables. The pioneering work of Bailey at the turn of the century yielded more than hundred variables, mostly RR Lyrae stars [Bailey(1902)]. By 1939, following discoveries of Shapley, Larink and Müller increased the number of catalogized variables in this cluster

^{*}e-mail: bakos@konkoly.hu

[†]Corresponding WWW: <http://www.konkoly.hu/staff/bakos/M3/>

to 201, though variability of several candidates was later refuted, and misidentifications were prevalent [Sawyer(1939), and references therein]. Observations of Sandage, Kurochkin, Kukarkin, Kholopov, Russev, Meinunger and Kaluzny led to the extension of later editions of the Variable Stars in Globular Clusters to 225 variables for M3 [Sawyer(1955), Sawyer(1973), and references therein], and recently to 238 entries [Clement(1998)].

However, erroneous identifications are present, partly because the coordinates respect to the cluster's (not uniformly accepted) central position were taken from various sources, partly due to the severe crowding conditions. Moreover, in some cases astrometry was carried out on photographic plates exposed under imperfect seeing conditions, and by manually centering on the stars' profiles. [Evstigneeva et al.(1994)] compiled a precise list of positions for all known or suspected variables using a *homogeneous* reference grid. As several new variable discoveries have sprung up since 1994, compilation of a new astrometric list with cross references became substantial.

This work is based on an observing campaign of M3 with a 0.9m Schmidt and a 1m RCC telescope, consisting of several observing runs in the spring seasons of 1998 and 1999. We primarily lay emphasis on identification and astrometry, but variability of the candidates is also confirmed in numerous cases. Photometric aspects and results on individual variables will be dealt with in forthcoming papers [Benkő et al.(2000), Bakos et al.(2000)].

2 Observations

As concerns the peripheral variables, we used CCD observations obtained with the 60/90/180cm Schmidt telescope at the Piszkestető Mountain Station of Konkoly Observatory. Observations in V-band were carried out on 11 nights evenly scattered in three months of the the spring season of 1998. The Kodak KAF-1600 1024×1536 chip yielded a $21' \times 28'$ field of view (FOV), with $\sim 1''/\text{pixel}$ resolution. Only the best seeing ($\sim 1.5''$) image was used for astrometry, but all of them were employed so as to verify the variability of the sources.

While identification of outer variables is straightforward in principle, crowding conditions impose difficulties in the inner few arcminutes. A subset of observations carried out with the 1m, f/13.6 RCC telescope at the same observatory was used to patch astrometry in the dense, inner region. The TH7896M UV-coated 1024×1024 CCD chip attached to the telescope yielded a FOV of $\sim 5' \times 5'$, with $0.288''/\text{pixel}$ resolution. The observing run in March 1999 produced time-

series data for 5 nights with strongly varying seeing conditions (ranging from $1.2''$ to $\gtrsim 2.5''$). Only the best night, and only V-filter observations were used in the present work.

As the innermost region of M3 was still not clearly resolved, we used archive Hubble Space Telescope (HST) Wide Field Planetary Camera 2 (WFPC2) observations¹ of M3 (proposed by Fusi Pecci, 1994, cf. Ferraro et al. 1997). This is the only set of publicly available WFPC2 observations where frames have short enough exposure times ensuring that RR Lyrae variables are not saturated. We used an F814W mosaic image with 3s integration time designated as “u2li010dt” in the archive.

The standard IRAF/CCDRED package was used for overscan and flatfield correction of the Schmidt and RCC images. The HST archive image was already calibrated by the HST pipeline, and while we were not performing direct photometry on the image, recalibration was needless.

3 Astrometry

All astrometric work was based on the USNO-A2.0 catalogue, which had been derived from PMM (Precision Measuring Machine) scans of POSS-I O and E plates [Monet(1996), Monet(1998)]. The typical astrometric error is about $0.15''$ for individual stars away from the plate corners and not in crowded fields. After thorough examination of crowding as a function of radial distance from the center of M3, we selected USNO-A2.0 stars with radial distance $r > 6'$ and brighter than $M_{red} = 17.8^m$ (hereafter *grid0*). Uncertainties in USNO astrometry of stars closer to the center might have led to considerable errors, ie. it was not possible to use USNO stars for reference in the RCC and HST fields. By careful choice of overlapping regions on the Schmidt, RCC and HST frames, the astrometric reference grid was extended towards the center. Equatorial coordinates given in the International Celestial Reference Frame (ICRF) were transformed to relative coordinates ($\Delta\alpha$ in $15 \times \text{seconds}^2$, $\Delta\delta$ in arcseconds) respect to the center³ of M3 (J2000.0): $\alpha_{M3} = 13^h 42^m 11.2^s$, $\delta_{M3} = 28^\circ 22' 32''$

¹ Based on observations made with the NASA/ESA Hubble Space Telescope, obtained from the data archive at the Space Telescope Science Institute. STScI is operated by the Association of Universities for Research in Astronomy, Inc. under NASA contract NAS 5-26555.

²This unit was chosen for convenience, as it has the same order of magnitude as arcseconds for small declinations. Values in Table 1 are given in *normal second* units.

³Note that this center slightly differs from the one accepted in [Clement(1998)] precessed for J2000.0

[Harris(1996)].

Using our self developed IRAF/GASTRO astrometric package⁴, we selected isolated, not saturated stars with $r > 6'$ on the Schmidt image (*grid1a*). The centers of these sources were determined by a script (GAST_MKGRID) built up from the IRAF/DAOFIND, PHOT, PSTSELECT programs.

Using a best estimate of the transformation between *grid0* and *grid1a* (initially a manual guess by GAST_CRUDE), stars were cross-identified, and transformations were refined. This iteration was done several times with variable rejection thresholds and fitting parameters, see-sawing back and forth between identification and refinement (GAST_PREC). Finally we fitted a second-order transformation between *grid0* (ICRF) and *grid1a* (Schmidt) of the form

$$\begin{aligned} X_{ICRF} &= A_{11} + A_{21}X_{Sch} + A_{12}Y_{Sch} + A_{31}X_{Sch}^2 + A_{22}X_{Sch}Y_{Sch} + A_{13}Y_{Sch}^2 \\ Y_{ICRF} &= B_{11} + B_{21}X_{Sch} + B_{12}Y_{Sch} + B_{31}X_{Sch}^2 + B_{22}X_{Sch}Y_{Sch} + B_{13}Y_{Sch}^2, \end{aligned}$$

which adequately conforms to the large-scale distortion of the Schmidt-camera field. The typical scatter of least-squares fits based on ~ 150 evenly scattered stars was lower than $0.13''$ rms, which is even better than the USNO-A2.0 precision itself.

As USNO-A2.0 astrometry is not reliable in RCC fields covering the dense center of the cluster ($5' \times 5'$), we extended our Schmidt grid to the innermost $3' > r > 1.5'$ ring (*grid1b*), and in a similar manner, established a grid on the RCC fields with $r > 1.5'$ (*grid2a*). The transformation between the two grids, based on 250 common stars, was derived similarly as previously mentioned, and had an overall scatter less than $0.04''$.

Finally, transformations were calculated between the RCC images (*grid2b*: $r < 1.5'$) and the HST PC, WF2, WF3, WF4 chips, using 70, 150, 150 and 200 stars, respectively. Scatter in the transformations was less than $0.04''$.

On the whole, it became possible to transform any astrometric position from the HST, RCC and Schmidt images to equatorial system (ICRF) with $\lesssim 0.15''$ precision.

4 Identification of variables

4.1 Tools

Four basic tools were applied to identify variables: coordinate lists, finding charts, variability images and light-curves. Relative coordinates for 238 variables

⁴All self-written software are available from the first author via request in e-mail.

are given in [Clement(1998)]. Unfortunately these coordinates are collected from several sources, thus far from being homogeneous, and the precision is only $\pm 0.1 - 1.0''$, which is not eligible for unambiguous identification in the center. Relative coordinates in right ascension are (traditionally) given in arcseconds as opposed to seconds, which involves a projection of the spherical equatorial coordinate system. [Evstigneeva et al.(1994)] give a more accurate list with proper equatorial coordinates. To be on the safe side, we used both lists to filter out misidentifications. New HST discoveries from [Guhathakurta et al.(1994)], properly transformed to equatorial system by [Goranskij(1994)] were also used. Finding charts are enclosed only in a few sources, such as [Kholopov(1963), Kholopov(1977)] and [Kaluzny et al.(1998)].

As concerns the variability images, we applied the Image Subtraction Method (ISM) for the best night on the RCC frames, and for all 11 nights on the Schmidt frames, as described in [Alard and Lupton(1998)] and [Alard(1999)]. After registering and convolving the images, then subtracting them from the reference frame with the aid of ISIS2.0, the resultant difference images were almost blank, only variable stars having negative or positive profiles. The variability image [Olech et al.(1999)] was the average of the absolute values of several difference frames, containing accumulated contributions from all variations respect to the reference frame, that is showing all sources variable on the timescale of the observations (~ 40 and 25 images for the Schmidt and RCC observations, respectively). In the case of the RCC observations, we restricted our investigation to variability detectable in one single night (mostly RR Lyraes and perhaps SX Phe stars), data reduction of subsequent frames will improve identification of both longer period (RGB) and fainter variables. On the other hand, the Schmidt observations spanning three months were also convenient for detecting long period irregular variables. It has to be emphasized that the primary goal was identification of the known variables and suspected ones, and not a complete variable search, although six new variables were found. In some complex cases (mostly close doubles) we also made use of scrutinizing the dependence of the light-curves on the (fixed) center of the photometry; the smaller scatter of the curve implies that the center of photometry is closer to the real position of the variable, which can serve as a criterion for selecting the truly varying star.

We implemented our IRAF/GISIS/GVARFIND task, which blinks the normal and the variability images, thus identification can be judged not only upon the initial coordinate-estimate but also on the variability of the source. This method seemed to be extremely useful in the central areas, where sometimes several candidates were equidistant from the corresponding rough position. The aforementioned task also performed fitting of an elliptical gauss profile to the

selected source, either on the normal image or on the variability image. If variability was sufficient, the latter case was preferred, as non-variable neighbors completely disappeared even in the dense regions, where profile-fitting would have been biased by overlapping profiles. It is worthy to note that HST variability image was not available, as we had only a single image with not saturated RR Lyrae stars.

In all cases identification meant determining the position of the variable by *precise psf-fitting*, and adequately *transforming* the coordinates to the ICRF.

Photometric accuracy is an important aspect when confirming variability or invariance of a star. Investigation of light curves derived by aperture photometry on the Schmidt and RCC frames yielded a crude estimate of the photometric errors being smaller than $\delta V \lesssim 0.05^m$ and $\delta V \lesssim 0.03^m$, respectively. However, significantly smaller accuracy could have been achieved in the most crowded fields.

As the Image Subtraction Method is less sensitive to crowding conditions, the accuracy of the (ISM) light curves we checked for variability were in the order of hundreds of mags in all cases. Variability of each star was checked and commented only if no light-curve had been previously given.

4.2 Finder charts

We present finder charts for 286 variables and suspected variables within the boundaries of the RCC frame (Figs. 1 to 10), or within the Schmidt frame (Figs. 11 to 15), to avoid further misidentifications and assist in any variability study of M3. Variables on the very edges of the Schmidt frame were omitted (V17, V92, V117), as well as variables denoted by “E” in Table 1 (V82, V91, V112, V113, V114, V115, V123, V141, V205, V206, V230). Although variable vZ1283 was identified on the edge of the RCC frame, the finder chart is given on the Schmidt image. Two HST variables (GU9016, GU9025) were not included as they were not readily visible on the RCC images (both identified from the HST frame). Several candidates revealed as doubles on the HST images were not resolved on the RCC frame, in which cases only one chart was given (V159a,b, V192a,b, KG8a,b, X14a,b). Though good quality finder charts for V237, V238 has been recently published by [Kaluzny et al.(1998)] they are repeated here for completeness.

Figures 1.-10 Caption: Finding charts for variables on the RCC frames. Boxes are approximately 15'' in width, North is up, East is to the left. Boxes from very sparse regions labeled as “WF” are 30'' wide. Different intensity

scales are chosen to reach the clearest resolution of each frame. (Note: figures are enclosed in png format for compression)

Figures 11.-15. Finding charts for variables on the Schmidt frames. Boxes are approximately $80''$ in width, North is up, East is to the left. (Note: figures are enclosed in png format for compression)

The revised positions and some additional information on the variables are given in Table 1. The IDs of the variables were extended in a similar manner to the [Clement(1998)] catalogue in case of all confirmed variables (column 1.). The last column gives all the crucial cross-references. The type of variability indicated in the second column of Tab. 1 was determined from our observations if light variation was detected. For some of the HST variables classification given by [Guhathakurta et al.(1994)] was adopted. Columns 3–5 and 6 give the relative coordinates and the observation used for the identification, respectively. Any comments of the individual stars are indicated in column 7.

Whenever possible, variables were identified on the HST image, as this yielded the most precise astrometry due to the $0.05''$ and $0.1''$ per pixel resolution for the PC and WF chips, respectively. Furthermore, due to the enhanced resolution, several variables turned out to be close double stars, in which cases original notation was split (eg. 122a, 122b)⁵. As we could not check variability on the HST frames, we tried to identify the variable component using the profile on the RCC variability frame. If a star was not within the WFPC2 boundaries, RCC images were checked, and in case the star was beyond these frames, Schmidt images were used. In eleven cases when variables were even outside the Schmidt frames, we accepted positions from [Evstigneeva et al.(1994)]. Still, our grid of variables remained self-consistent, as our coordinates are compatible with [Evstigneeva et al.(1994)] in the sense that no discernible offset is present (see later).

Kholopov variables (X) were manually selected with GVARFIND using finder charts in [Kholopov(1963), Kholopov(1977)] and our variability image. Some of the Kholopov variables were already included in [Clement(1998)], without firm constraints on their light-curves. All these cases were checked for variability. We identified the remaining 11 suspected candidates, and confirmed variability of five of them.

[Kadla and Gerashchenko(1980)] variables (KG) were identified from the list

⁵Notation was also splitted in case more than one candidates were equidistant from the position given in previous references, and identification was dubious.

in the original paper, and from [Evstigneeva et al.(1994)]. Variability of several candidates is confirmed, and new ID numbers are given.

All von Zeipel (vZ) candidates listed in [Evstigneeva et al.(1994)] were identified on the RCC and Schmidt images. As all of them were suspected as long-period variables [Welty(1985), Meinunger(1980)], variability was checked on the Schmidt frames. Variability is ascertained only in one case (vZ297), while six other candidates remain suspected variables. The remaining stars are constant within the photometric errors of the Schmidt measurements.

Sandage variables (S-) were identified with the aid of finder charts in [Sandage(1953)]. Except for S-AQ, S-I-II-52, S-I-II-54, these stars were suspected as bright, long-period variables [Meinunger(1980)], however all, but one (S-I-VI-65) proved to be constant on the Schmidt frames. Bao-An et al. (1993a,b) and [Bao-An et al.(1994)] drew attention to three new short-period, low-amplitude variables (S-I-II-52, S-I-II-54, S-AQ). These stars were identified from charts in [Sandage(1953)], but low amplitude variability has not yet been confirmed on the Schmidt images.

[Guhathakurta et al.(1994)] gave a list of variable stars (GU) in the center of M3 using HST/WFPC observations, giving unique ID numbers, relative coordinates respect to star AC999, rough average magnitudes, and classification. The list was appropriately transformed by [Goranskij(1994)] to match [Evstigneeva et al.(1994)], and cross-identification showed that only 11 out of the 40 variables were new discoveries. By performing the same analysis, we reduced the number of new HST discoveries to 9 (confer revised cross-references in Table 1). Variability is confirmed except for GU1711 (long-period suspected variable) and GU9016 (faint SX Phe star).

Three prominently variable RR Lyrae stars were found on the RCC images, and three long-period variables on the Schmidt images, without any previous reference. These supposedly new variables are listed at the end of Table 1. Preliminary light-curves for the newly discovered variables 269–274 are presented in Fig. 16.

Coordinates in the resultant list were correlated with the original list of [Clement(1998)], and with the exception of few misidentifications and defective coordinates in the above reference (V146, V151, V165, V181, V196, V199, V204), the overall scatter of the fits was $\sim 1''$ rms. Correlation with the list of [Evstigneeva et al.(1994)] yielded considerably more precise fits with $\lesssim 0.2''$ rms. This reinforces the *absolute* precision of our astrometry being better than $0.2''$, even with taking the uncertainties rising from the USNO-A2.0 catalogue into account. As concerns relative astrometry, our grid is self-consistent within the error of $\sim 0.15''$.

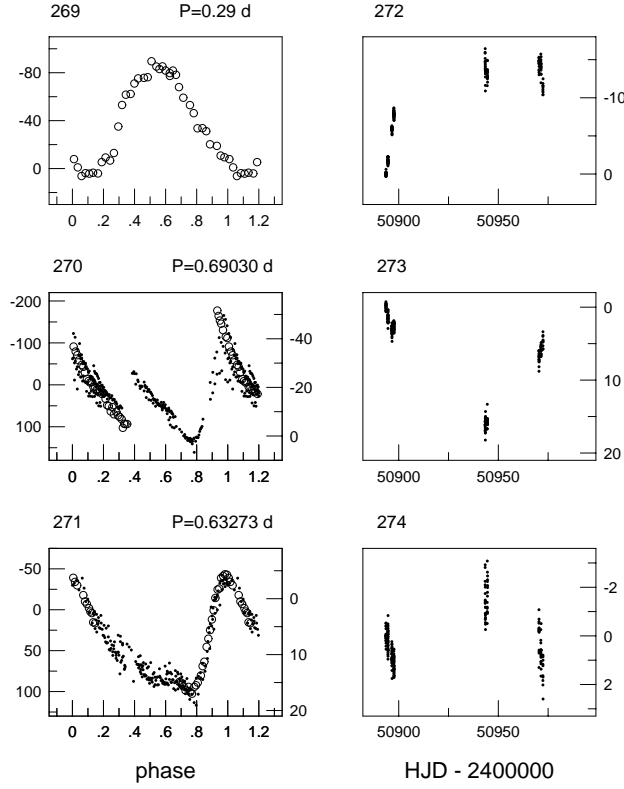


Figure 16: Light-curves obtained using image subtraction method (ISIS2.0) of the new variables. The RR Lyraes (V269–V271) are located in the inner part of M3; both the 1m RCC (denoted by open circles) and Schmidt observations (dots) are plotted. Scales (in units of differential fluxes (ADU/s) normalized with a factor of 1000) are shown on the left and right axes, respectively. The large scatter and the jump in the light-curve of V270 are supposed to be defect caused by the inappropriate resolution of the Schmidt images in a very dense region (see Fig. 9). For long period variables (V272–V274) lying in the outer region of the cluster only Schmidt data was available.

Acknowledgments

We are grateful to Dr. Béla Szeidl for his persevering help and expertise in M3 variables. This project was supported by OTKA grants T-24022 and T-30954.

Table 1: List of variables and suspected variables in M3^a

ID ^b	Type	$\Delta\alpha(sec)$	$\Delta\alpha('')$ ^c	$\Delta\delta('')$	Tel. ^d	Comm. ^e	Cross-ref. ^f
1	RRab	-0.071	-0.93	-118.12	R		
2	not var.	1.516	20.01	63.28	H	ckn	
3	RRab	4.510	59.52	-50.41	R		
4n	RRab	-3.006	-39.68	1.53	H	d	GU9003
4s	RRab	-2.983	-39.37	1.16	H	d	GU9004
5	RRab	20.089	265.13	-11.14	S		
6	RRab	-9.098	-120.07	69.71	R		
7	RRab	-0.102	-1.35	98.39	H		
8	RRab	-5.904	-77.92	-13.19	R	f	
9	RRab	-21.685	-286.19	-198.45	S		
10	RRab	11.905	157.11	148.71	S		
11	RRab	-11.207	-147.91	-199.99	S		
12	RRc	0.064	0.85	-134.77	S		
13	RRab	-1.611	-21.27	-127.31	S		
14	RRab	-3.381	-44.62	-150.70	S		
15	RRab	-6.519	-86.04	-263.30	S		
16	RRab	-22.480	-296.69	-83.69	S		
17	RRab	11.213	147.98	-429.23	S	e	
18	RRab	7.755	102.36	-284.70	S		

^aCenter for M3 is adopted from [Harris(1996)]: $\alpha_{M3} = 13^h42^m11.2^s$, $\delta_{M3} = 28^\circ22'32''$ (J2000.0)

^bNumeric identification 1 to 238 were listed in [Clement(1998)] and 239 to 274 is added in this work. If the star turned out to be double on HST images, notation is splitted to "a,b...", etc. The same notation is used if there are more than one candidates.

^cThis column is given for compatibility with previous works, assuming a projection from seconds to arcseconds using the accepted center of the cluster.

^dTelescope used for identification: H – HST/WFPC2, R – RCC, S – Schmidt, E – coordinates from [Evstigneeva et al.(1994)]

^eComments are: "c" – extra comment on the star, "d" – double star, "e" – on the edge of frame, "f", "f?" – variability confirmed and suspected from corresponding RCC variability image and light curve, "i" – identification problems, "j", "j?" – variability confirmed and suspected on Schmidt images, "k" – not variable on Schmidt images, "m" – merging with closeby star, "n" – variability not detected on RCC images.

^f"X" stands for [Kholopov(1963), Kholopov(1977)], "KG" for [Kadla and Gerashchenko(1980)], "GU" for [Guhathakurta et al.(1994)], "S" for [Sandage(1953)], "Sh" for [Shapley(1914)], "vZ" for [von Zeipel(1908)], "B" for the present work. The vZ and Sandage numbers were omitted, if not crucial.

Table 1: (continued)

ID	Type	$\Delta\alpha(sec)$	$\Delta\alpha('')$	$\Delta\delta('')$	Tel.	Comm.	Cross-ref.
19	RRab	26.912	355.17	-234.12	S		
20	RRab	25.626	338.21	-260.15	S		
21	RRab	26.579	350.79	29.71	S		
22	RRab	14.717	194.23	0.15	S		
23	RRab	-8.349	-110.19	288.91	S		
24	RRab	-10.881	-143.60	20.11	S		
25	RRab	-9.111	-120.24	-21.66	R		
26	RRab	-13.149	-173.54	-33.40	S		
27	RRab	-8.019	-105.83	-92.68	R		
28	RRab	-1.566	-20.66	-95.40	R		
29	RRab	-4.608	-60.81	-63.42	R	c	
30	RRab	-2.467	-32.55	68.13	H		
31	RRab	2.786	36.77	75.62	H		
32	RRab	1.197	15.79	70.53	H		
33	RRab	5.639	74.43	-78.52	R		
34	RRab	10.523	138.88	180.72	S		
35	RRab	-7.753	-102.32	-268.37	S		
36	RRab	13.344	176.11	-24.40	S		
37	RRc	-17.633	-232.72	173.81	S		
38	RRab	-15.146	-199.90	137.16	S		
39	RRab	-18.223	-240.50	130.63	S		
40	RRab	-20.257	-267.35	121.21	S		
41	RRab	-6.803	-89.79	63.91	R		
42	RRab	-5.676	-74.91	50.59	H		
43	RRab	7.873	103.90	35.09	R		
44	RRab	13.171	173.83	110.21	S		
45	RRab	-17.959	-237.02	-120.53	S		
46	RRab	-9.373	-123.71	-41.30	R		
47	RRab	-8.578	-113.21	-63.05	R		
48	RRab	9.968	131.56	-91.57	R		
49	RRab	10.915	144.06	-89.23	R	e	
50	RRab	1.046	13.81	-223.96	S		
51	RRab	2.677	35.34	-215.88	S		
52	RRab	-5.565	-73.45	161.47	S		

Table 1: (continued)

ID	Type	$\Delta\alpha(sec)$	$\Delta\alpha('')$	$\Delta\delta('')$	Tel.	Comm.	Cross-ref.
53	RRab	-0.263	-3.48	132.94	R		
54	RRab	-2.207	-29.12	116.60	R		
55	RRab	-15.271	-201.54	333.78	S		
56	RRc	-10.511	-138.72	367.92	S		
57	RRab	12.060	159.17	10.35	S		
58	RRab	-6.245	-82.42	56.12	R		
59	RRab	-7.951	-104.94	-218.58	S		
60	RRab	-22.135	-292.14	-306.30	S		
61	RRab	14.595	192.63	373.81	S		
62	RRab	7.031	92.79	427.27	S		
63	RRab	3.037	40.08	352.17	S		
64	RRab	8.919	117.72	340.62	S		
65	RRab	9.727	128.38	338.11	S		
66	RRab	-7.409	-97.78	131.00	R		
67	RRab	-9.676	-127.70	132.51	R		
68	RRd	1.907	25.16	185.18	S		
69	RRab	6.379	84.19	151.44	R	e	
70	RRc	3.143	41.47	162.56	S		
71	RRab	12.456	164.39	8.52	S		
72	RRab	34.041	449.26	9.47	S		
73	RRc	33.506	442.20	73.93	S	j	
74	RRab	6.952	91.75	161.16	S		
75	RRc	3.943	52.03	169.47	S		
76	RRab	-0.779	-10.28	-77.78	R		
77	RRab	-6.902	-91.10	37.86	R		
78	RRab	3.859	50.93	76.95	H		
79	RRd	3.521	46.47	359.70	S		
80	RRab	31.828	420.06	295.95	S		
81	RRab	26.173	345.43	362.34	S		
82	RRab	-7.300	-96.34	-591.36	E		
83	RRab	-33.191	-438.05	121.73	S		
84	RRab	5.123	67.61	175.27	S		
85	RRc	23.454	309.54	237.22	S		
86	RRc	39.189	517.20	-102.83	S		

Table 1: (continued)

ID	Type	$\Delta\alpha(sec)$	$\Delta\alpha('')$	$\Delta\delta('')$	Tel.	Comm.	Cross-ref.
87	RRd	8.663	114.34	70.73	R		
88	RRc	-2.355	-31.07	-59.58	R		
89	RRab	2.419	31.93	-100.32	R		
90	RRab	7.725	101.96	-177.72	S		
91	RRab	-0.621	-8.19	-539.94	E		
92	RRab	-1.807	-23.84	-398.40	S	e	
93	RRab	-23.787	-313.94	-387.62	S		
94	RRab	-36.648	-483.67	-216.49	S		
95	long per.	-11.427	-150.81	25.28	S		
96	RRab	-12.067	-159.26	-224.36	S		
97	RRc	-9.487	-125.21	-187.13	S		
98	not var.	10.326	136.28	7.29	R	ekn	
99	RRd	15.563	205.39	-43.93	S		
100	RRab	5.566	73.46	108.02	R		
101	RRab	3.795	50.08	93.85	R		
102	not var.	4.693	61.94	125.36	R	kn	
103	not var.	4.708	62.13	130.70	R	kn	
104	RRab	-1.687	-22.27	155.46	R		
105	RRc	-1.335	-17.61	201.42	S		
106	RRab	-3.393	-44.78	178.09	S		
107	RRc	-5.551	-73.26	344.84	S		
108	RRab	-16.408	-216.55	320.08	S		
109	RRab	-6.457	-85.21	12.52	H		
110	RRab	-7.259	-95.81	-5.71	R		
111	RRab	-6.735	-88.89	31.90	H		
112		-10.400	-137.26	-709.31	E		
113	RRab	15.646	206.49	-679.26	E		
114	RRab	1.025	13.53	631.56	E		
115	RRab	33.913	447.57	675.49	E		
116	RRab	-37.143	-490.20	473.05	S		
117	RRab	7.198	95.00	-457.98	S	e	
118	RRab	11.306	149.22	-281.42	S		
119	RRab	19.473	257.01	117.00	S		
120	RRab	-22.199	-292.98	240.28	S		

Table 1: (continued)

ID	Type	$\Delta\alpha(sec)$	$\Delta\alpha('')$	$\Delta\delta('')$	Tel.	Comm.	Cross-ref.
121	RRab	-3.027	-39.95	65.91	H		
122a	RRab	-2.148	-28.35	-36.74	R	cm	GU9007
122b		-2.231	-29.45	-36.36	R	cm	
123	RRab	-18.941	-249.98	-988.00	E		
124	RRab	-4.671	-61.65	-191.15	S		
125	RRc	14.449	190.69	-121.86	S		
126	RRc	-0.837	-11.04	-136.10	S		
127		7.364	97.19	-50.42	R	cn	
128	RRc	8.926	117.80	141.70	R		
129	RRc	-2.986	-39.41	87.55	H		
130	RRab	0.577	7.61	94.30	H		
131	RRc	-5.289	-69.81	37.27	H		
132	RRc	-3.757	-49.58	-11.85	H		GU9001
133	RRab	-4.176	-55.12	54.18	H		
134	RRab	-1.409	-18.60	62.87	H		
135	RRab	-1.747	-23.06	48.69	H		
136	RRab	-1.625	-21.44	44.33	H	f	
137	RRab	4.275	56.42	-8.71	H		
138	long per.	-19.662	-259.49	50.72	S		
139	RRab	2.916	38.49	38.60	H		
140	RRc	-0.901	-11.90	119.17	H		
141	EW	-113.050	-1492.00	-250.67	E		RV CVn
142	RRab	-1.934	-25.53	-48.12	R		Sh2, GU9009
143	RRab	-2.294	-30.27	27.22	H		GU9005
144	RRab	4.406	58.15	-89.10	R		
145	RRab	2.421	31.95	19.18	H	m	
146	RRab	7.301	96.37	-47.91	R	c	
147	RRc	-1.364	-18.00	57.57	H		
148	RRab	-0.239	-3.16	48.21	H		
149	RRab	2.903	38.32	63.43	H		
150	RRab	5.487	72.42	48.61	H		
151	RRab	0.789	10.42	-30.86	R	c	
152	RRc	6.269	82.74	61.77	R		
153	not var.	-2.585	-34.12	71.71	H	kn	

Table 1: (continued)

ID	Type	$\Delta\alpha(sec)$	$\Delta\alpha('')$	$\Delta\delta('')$	Tel.	Comm.	Cross-ref.
154	W Vir	0.463	6.10	-18.26	H	cm	GU9024
155	RRc	-4.500	-59.39	-64.74	R	c	Sh1
156	RRab	-1.212	-15.99	-30.39	R	c	GU9019?
157	RRab	-1.013	-13.36	46.13	H		
158	not var.	-0.857	-11.30	-29.49	R	ckn	
159a	RRab	-0.842	-11.12	26.90	H	cd	
159b		-0.833	-11.00	26.67	H	cd	
160	RRab	-0.394	-5.20	-32.75	R		GU9021
161	RRab	1.611	21.27	-46.98	R	c	
162	not var.	2.404	31.73	-20.75	R	kn	
163	not var.	-0.903	-11.92	-21.25	R	cn	
164		1.890	24.94	-25.18	R	j?	
165	RRab	5.846	77.16	31.01	H	c	
166	RRd	-7.031	-92.79	2.69	R		
167	RRab	-5.613	-74.08	-26.25	R		
168	RRc	-3.121	-41.18	17.65	H		GU9002
169	not var.	-1.918	-25.31	-23.85	R	kn	
170	RRc	-1.863	-24.59	43.45	H	c	
171	RRc	-1.686	-22.25	27.40	H		Sh3
172	RRab	-1.293	-17.07	36.67	H		
173	RRab	-0.691	-9.13	49.66	H		
174	RRab	-0.367	-4.85	-23.30	R		GU9022
175	RRab	3.437	45.35	37.17	H		
176	RRab	3.783	49.93	43.95	H		
177	RRc	5.068	66.89	-18.21	R		
178	RRc	6.279	82.86	57.72	R		
179		?	?	?		ci	
180	RRab	-1.111	-14.66	-18.53	R	cfi	Sh5?
181	RRab	-2.001	-26.40	-2.98	H	cf	GU9008
182	not var.	-1.076	-14.20	70.47	H	kn	
183	not var.	2.580	34.05	17.63	H	kn	
184	RRab	-1.624	-21.43	-4.35	R		GU9013
185		-0.883	-11.66	41.84	H	cn	
186	RRab	1.301	17.18	-52.32	R		

Table 1: (continued)

ID	Type	$\Delta\alpha(sec)$	$\Delta\alpha('')$	$\Delta\delta('')$	Tel.	Comm.	Cross-ref.
187	RRab	-1.550	-20.46	19.82	H	m	
188	RRc	-1.704	-22.49	34.72	H		
189	RRab	-1.611	-21.27	-10.18	R		Sh4, GU9014
190	RRab	-0.319	-4.22	39.16	H		
191	RRab	0.426	5.62	33.81	H	m	
192a	RRab	0.112	1.48	14.87	H	cd	
192b		0.112	1.48	14.74	H	cd	
193	RRab	1.401	18.50	3.63	H		GU2538
194	RRab	1.550	20.45	-1.98	H	cm	KG10
195	RRab	-0.708	-9.35	-17.29	R		GU9020
196a	not var.	3.848	50.79	11.60	H	cikn	
196b	not var.	3.811	50.30	12.22	H	cikn	
196c	not var.	3.915	51.67	13.18	H	cikn	
197	RRab	4.713	62.19	20.03	H		
198		-1.449	-19.13	25.74	H	cn	
199	RR	-1.168	-15.42	21.92	H		
200	RRab	-0.021	-0.28	31.95	H	cfm	
201	RRab	0.585	7.73	1.82	H		GU1600
202	RRc	-28.355	-374.23	105.76	S		
203	RRc	-1.751	-23.11	-301.59	S		
204	not var.	-7.583	-100.09	-12.08	R	ckn	
205	RRab	-83.596	-1103.28	653.86	E		WY CV _n
206	RRab	9.113	120.27	-1720.86	E		WZ CV _n
207	RRc	3.017	39.82	-20.66	R	f	X3
208	RRc	0.509	6.71	-47.73	R	f	X4
209	RRc	-4.836	-63.82	-89.17	R	cf	X6
210	RRc	-6.213	-82.00	0.35	H	fm	X8
211	RRab	-3.797	-50.11	17.17	H	cd	X9
212	RRab	-1.329	-17.53	-27.78	R		X11, GU9017
213	RRc	-1.630	-21.51	-19.40	R		X12, GU9011
214	RRab	2.734	36.08	16.70	H		X15
215	RRab	-0.759	-10.02	9.52	H		X16, GU238
216	RRc	2.399	31.67	-0.59	H	f	X19
217	RRab	0.278	3.67	-16.43	H		X27, GU9023

Table 1: (continued)

ID	Type	$\Delta\alpha(sec)$	$\Delta\alpha('')$	$\Delta\delta('')$	Tel.	Comm.	Cross-ref.
218	RRab	2.424	31.99	-19.01	R		X28
219	RRab	-4.139	-54.62	25.72	H	fm	X29
220	RRab	2.801	36.97	-5.50	H	f	X31
221	RRc	-0.985	-12.99	-3.19	H		X32, GU85
222	RRab	7.565	99.84	-52.96	R		X34
223	RRc	2.083	27.49	4.46	H	f	X37
224		-1.375	-18.15	15.16	H	f?m	X38
225	long per.	0.863	11.38	234.63	S		
226	RRab	1.783	23.54	-8.04	R		X39
227	not var.	-8.048	-106.21	-51.40	R	kn	X7
228	not var.	-2.229	-29.41	46.80	H	kn	X10
229	RRab	-2.194	-28.95	-35.13	R	cm	X40, GU9006
230		19.733	260.44	-482.84	E		X41
231	not var.	9.731	128.42	57.73	R	kn	X42
232	not var.	9.310	122.87	52.22	R	kn	X43
233		2.618	34.55	3.03	H	n	X44
234	RRab	1.889	24.93	-29.30	R	f	X47
235	RRab	2.573	33.95	47.61	H	f	X49
236	long per.	30.337	400.38	-203.99	S	j	vZ1397
237	SX Phe	1.757	23.19	-170.11	S	c	
238	EW	4.551	60.06	-254.85	S	c	
239	RRab	-1.326	-17.50	-16.28	R	ci	X13, GU9018, Sh5?
240	RRc	-1.739	-22.95	3.10	H	cd	X14a, GU9010
		-1.713	-22.61	3.00	H	cd	X14b, GU9010?
241	RRab	-0.435	-5.74	5.78	H	cm	X17, GU507
		-0.326	-4.30	2.23	H	cn	X18
242	RRab	2.009	26.52	-7.63	R	cfm	X20
243	RRab	1.071	14.13	-16.33	R		X22, GU9026
244	RRab	-1.575	-20.78	14.41	H	cf	X23
245	RRc	-1.300	-17.16	27.85	H	f	X25
246	RRc	1.562	20.62	8.33	H	f	X30
247	RRab	3.593	47.43	-16.32	R	df	X35
248	RRab	-1.532	-20.22	17.52	H	c	X36, GU9015
249	RRab	-0.887	-11.71	16.07	R	cf	KG1

Table 1: (continued)

ID	Type	$\Delta\alpha(sec)$	$\Delta\alpha('')$	$\Delta\delta('')$	Tel.	Comm.	Cross-ref.
250	RRab	-0.642	-8.48	19.92	H	cdf	KG2
251	RR	-0.245	-3.23	1.79	H	cim	KG3, GU684
252	RRab	-0.202	-2.67	11.79	H		KG4, GU734
		0.504	6.65	-6.38	R	cn	KG5
		0.871	11.49	13.66	H	kn	KG6
253	RRc	0.942	12.44	0.62	H		KG7, GU2042
254	RRab	1.217	16.06	21.39	H	cdfm	KG8a
		1.258	16.60	21.03	H	cdfm	KG8b
255	RR	1.409	18.59	11.81	H	f	KG9
256	RRc	1.896	25.03	26.58	H	cdf	KG11
257	RRab	1.857	24.50	-3.80	R	f	KG12
		2.335	30.82	-30.71	R	cin	KG13
258	RR	3.112	41.07	59.38	H	f	KG14
259	RRc	3.373	44.51	22.70	H	cdfj	KG15
		-6.320	-83.41	-88.45	R	k	KG16
		6.080	80.24	265.22	R	k	KG17, S-I-II-53
		-34.879	-460.32	-67.45	S	j?	vZ177
		-26.927	-355.38	212.99	S	k	vZ194
		-18.005	-237.62	-186.21	S	j?	vZ250
		-16.158	-213.25	-196.90	S	k	vZ265
		-14.865	-196.19	204.76	S	j?	vZ281
260	long per.	-13.023	-171.88	-399.92	S	j	vZ297
		-7.963	-105.10	41.71	R	ckn	vZ380
		1.175	15.50	-234.43	S	j?	vZ853
		4.137	54.59	97.54	S	cn	vZ1066
		11.379	150.18	-45.84	R	ckn	vZ1283
		17.607	232.37	104.86	S	j?	vZ1345
		20.205	266.67	22.55	S	j?	vZ1360
		-11.823	-156.04	217.50	S	k	S-I-III-38
		-12.881	-170.00	-302.20	S	k	S-O
		-9.852	-130.03	209.23	S	k	S-AK
		14.830	195.72	268.75	S	k	S-I-I-27
		12.720	167.87	-77.30	S	j?	S-I-VI-65
		3.878	51.18	273.98	S	ck	S-AQ

Table 1: (continued)

ID	Type	$\Delta\alpha(sec)$	$\Delta\alpha('')$	$\Delta\delta('')$	Tel.	Comm.	Cross-ref.
		5.147	67.92	267.31	S	ck	S-I-II-52
		5.910	78.00	261.32	S	ck	S-I-II-54
261	RRc	-1.113	-14.69	8.18	H		GU32
262	RR	-0.384	-5.07	5.28	H	c	GU552
263	SX Phe	-0.329	-4.35	-7.82	H	c	GU576
264	RRc	-0.329	-4.35	-2.31	R		GU586
265	RRab	0.512	6.76	-16.36	H	cm	GU1489
		0.673	8.87	5.73	H	cn	GU1711
266	RRc	-1.648	-21.75	12.14	H		GU9012
267	SX Phe	-1.416	-18.69	15.87	H	cm	GU9016
268	RRab	0.512	6.76	-17.80	H	cm	GU9025
269	RRc	1.590	20.98	0.88	R	m	B1
270	RRab	0.746	9.85	59.97	R	m	B2
271	RRab	0.992	13.09	45.84	R	m	B3
272	long per.	2.087	27.54	-161.58	S		B4
273	long per.	-4.469	-58.98	-95.07	S		B5
274	long per.	0.901	11.89	-71.47	S		B6

A Notes on individual stars

V2: Two closeby candidates in [Evstigneeva et al.(1994)] (hereafter ESTS94); none of them is variable. From charts in [Kholopov(1963), Kholopov(1977)] (hereafter K63 and K77) it is not obvious which star is marked as “2”. Original positions from [Sawyer(1973)] (hereafter SH73) and [Clement(1998)] (hereafter CC98) are closer to the west candidate.

V29: Positions of V29 and V155 are interchanged in ESTS94.

V122: Two candidates; V122a is more likely the true variable, based upon its light-curve. Merging with V229.

V127: CC98 position merges with position of V222. K77 gives correct identification.

V146: CC98 position is $\sim 4''$ away from the variable. As V127 and V222 are closeby, this position error might be misleading. Identification confirmed from K77 charts.

V151: Quite far ($\sim 3''$) from the CC98 position, the same star is marked in K77. No other candidate.

V154: W Vir star, merging with an RR Lyrae V268.

V155: Positions of V29 and V155 are interchanged in ESTS94.

V156: Formal position of GU9019 is $1.3''$ away from V156, not coinciding with any star. It is likely to be the same variable as V156.

V158: Despite the entry in CC98, it doesn't seem to be variable on the RCC images (one night), neither on the Schmidt images.

V159: Double on HST/WF2 images: V159a, V159b. Not possible to select the variable component.

V161: Misidentified in ESTS94 (with non-variable star in $\sim 2''$ distance).

V163: Star from [Müller(1933)]; identification is dubious, position is equidistant from a non-variable and a variable star (later V180). K63 and K77 marks the non-variable candidate as 163. CC98 says V163 is not var. The not variable candidate is accepted as V163, in order to avoid confusion.

V165: The coordinates in SH73, CC98 are erroneous (sign on declination offset is “-” instead of “+”).

V170: Elongated profile on HST/WF2 image. Maybe double?

V179: This candidate is very far from the cluster, only crude position is known, charts are not available. Three stars are equidistant on the POSS images from the quoted position. CC98 notes that this star is non-variable.

V180: Two equidistant candidates close to SH73 (Sh) position: one is the same as X13=(V239), which is variable indeed. K77 marks the other star as 180, and announces X13 as a new variable. Shapley says that V180 is non-variable. For convenience, the candidate shown in K77 is chosen to be V180. Variability is confirmed, as opposed to CC98.

V181: Appropriately transformed CC98 position coincides with a variable star. However, CC98 notes that this star is not variable. K77 finder charts mark a closeby, non-variable star as 181. ESTS94 identifies the same star as V181. We propose that both K77 and ESTS94 identifications are erroneous, and V181 is variable, identical to GU9008. Faint companion to the NW on HST/WF2 image.

V185: No variable star in the vicinity of the position in CC98. V185, as identified in ESTS94 shows no variability.

V192: Obviously double on HST/PC image; not possible to select the variable.

V194: Two candidates on HST/PC frame. Merging with other stars to the N in a NS chain, all of them showing variability? Time-series observations with better seeing would be needed for firm identification. Formal position of KG10, as derived from [Kadla and Gerashchenko(1980)] (hereafter KG80) and ESTS94, is merging with V194.

V196: CC98 position is close to a constant star, but it is not the same as the one marked in K77 finder charts. The latter is also constant (196c). The star close to the CC98 position, is a double star on the HST/WF4 image (196a, 196b), both components are constant.

V198: Despite the entry in CC98 and the short period ($\sim 0.2797^d$), it doesn't seem to be variable on the RCC images (one night).

V200: Misidentified in ESTS94, merging with a brighter star.

V204: Roughly $6''$ away from the position in CC98; identification from K77 chart. No significant variability detected on the RCC frames (one night), neither on the Schmidt frames.

V209: ESTS94 lists two stars at the position. Unfortunately the area is not within the HST fields. Variable is more likely to be the southern one (from variability image).

V211: Obviously double on HST images.

V229: Merging with V122a and V122b.

V237, V238: Too faint stars for variability to be confirmed on Schmidt images.

V239=X13: Confer comments at V180.

V240=X14: Obviously double on HST/WF2 images: X14a, X14b. Maybe both components are variable, as the source is elongated on the variability image.

V241=X17: See comment at V262.

X18: K77 marks a relatively bright star as X18, which shows no significant variability on the RCC frames spanning one day. Very close to formal position of V251 (=KG3).

V242=X20: Merging with a bright star, and close to V257.

V244=X23: Two candidates on HST/WF2 image: the true variable was selected using the RCC variability image. X23 is not identical with GU9012, as proposed by [Goranskij(1994)].

V248=X36: Elongated profile on HST/WF2 image.

V249=KG1: Identification with the help of KG80 positions adequately transformed to our system.

V250=KG2: Two close candidates on HST/WF2 image.

V251=KG3: Merging with X18, only resolved on HST/PC frames. Variability (due to the extreme crowding) not detected unambiguously.

KG5: Bright star, identified using both ESTS94 and KG80: no significant variability.

V254=KG8: Two candidates on HST/WF4 image, merging on ground-based images. Light curves are almost the same for the two slightly different positions. Further investigation in good seeing would be needed to draw firm conclusion.

V256=KG11: Two candidates on HST/WF4 images; the true variable was selected using the RCC variability image.

KG13: Identification dubious; two bright stars and a fainter companion close to the position showing no significant variability.

V259=KG15: Two candidates on HST/WF4 images; the true variable was selected using the RCC variability image.

vZ380: Star in ESTS94, variability from [Meinunger(1980)] – obj. a.

vZ1066: Star in ESTS94, variability from [Meinunger(1980)] – obj. b.

vZ1283: Star in ESTS94, variability from [Meinunger(1980)] – obj. c.

S-AQ, S-I-II-52, S-I-II-54: Low amplitude variability [Bao-An et al.(1993a)], [Bao-An et al.(1993b)], [Bao-An et al.(1994)] is not detected on the Schmidt images.

V262=GU552: This might be a very close companion to V241, only resolved on HST images. Light curve is almost identical to that of the closeby V241, due to merging. No trace of RRc variation is detectable in the light-curve, in spite of comments in [Guhathakurta et al.(1994)]. Higher resolution time-series observations would be needed to conclude more on its variability.

V263=GU576: SX Phe, barely visible on the 1m RCC images. Position from HST data. Elongated on HST/WF2?

V265=GU1489: RR Lyrae, merging with V154 and V268.

GU1711: Suspected variable in [Guhathakurta et al.(1994)], constant on the RCC images.

V267=GU9016: SX Phe star merging with V224, resolved on the HST/WF2 frame.

V268=GU9025: RR Lyrae star merging with V154 (W Vir) and V265.

References

- [Alard and Lupton(1998)] Alard, C. and Lupton, R. H. 1998 ApJ 503 325
- [Alard(1999)] Alard, C. 1999 A&A 343 10
- [Bailey(1902)] Bailey, S. I. 1902 Harvard Ann., 38 238
- [Bakos et al.(2000)] Bakos, G. Á. et al., in preparation

- [Bao-An et al.(1993a)] Bao-An, Yao, Zhang Chun-Seng and Qin Dao 1993a IBVS No 3955
- [Bao-An et al.(1993b)] Bao-An, Yao, Zhang Chun-Seng and Qin Dao 1993b IBVS No 3962
- [Bao-An et al.(1994)] Bao-An, Yao, Zhang Chun-Seng and Qin Dao 1994 IBVS No 4003
- [Benkő et al.(2000)] Benkő, J. M. et al. in preparation
- [Clement(1998)] Clement, C. M. 1998 personal communication
- [Evstigneeva et al.(1994)] Evstigneeva, N. M., Samus', N. N., Tsvetkova, T. M. and Shokin, Y. A. 1994 Pisma Astron. Zh. 20 693
- [Ferraro et al.(1997)] Ferraro, F. R., Paltrinieri, B., Fusi Pecci, F., Cacciari, C., Dorman, B. and Rood, R. T. 1997 ApJ 484 L145
- [Goranskij(1994)] Goranskij, V. P. 1994 IBVS No 4129
- [Guhathakurta et al.(1994)] Guhathakurta, P., Yanny, B., Bahcall, J. N. and Schneider, D. P. 1994 AJ 108 1786
- [Harris(1996)] Harris, W.E. 1996, AJ, 112, 1487
- [Kadla and Gerashchenko(1980)] Kadla, Z. I. and Gerashchenko, A. N. 1980 Astron. Tsirk. No 1123 1
- [Kaluzny et al.(1998)] Kaluzny, J., Hilditch, R. W., Clement, C. and Rucinski, S. M. 1998 MNRAS 296 347
- [Kholopov(1963)] Kholopov, P. N. 1963 Perem. Zvezdy 14 275
- [Kholopov(1977)] Kholopov, P. N. 1977 Perem. Zvezdy, 20 313
- [Meinunger(1980)] Meinunger, I. 1980 Mitteil. Veränderliche Sterne, Sonneberg 8 159
- [Monet(1996)] Monet, D. G. 1996 BAAS 28 905
- [Monet(1998)] Monet, D. G. 1998 BAAS 30 1427
- [Müller(1933)] Müller, Th. 1933 Veröff. Berlin-Babelsberg 11 1

- [Olech et al.(1999)] Olech, A., Woźniak, P. R., Alard, C., Kaluzny, J. and Thompson, I. B. 1999 MNRAS 310 759
- [Pickering(1889)] Pickering, E. C. 1889 Astr. Nach. 123 207
- [Sandage(1953)] Sandage, A. R. 1953 AJ 58 61
- [Sawyer(1939)] Sawyer, H. B. 1939 Publ. David Dunlop Obs. 1 4
- [Sawyer(1955)] Sawyer, H. B. 1955 Publ. David Dunlop Obs. 2 2
- [Sawyer(1973)] Sawyer, H. B. 1973 Publ. David Dunlop Obs. 3 6
- [Shapley(1914)] Shapley, H. 1914 ApJ 40 443
- [Welty(1985)] Welty, D. E. 1985 AJ 90 2555
- [von Zeipel(1908)] von Zeipel, M. H. 1908 Ann. Obs. Paris 25 1

This figure "Fig1.png" is available in "png" format from:

<http://arxiv.org/ps/astro-ph/0004259v1>

This figure "Fig2.png" is available in "png" format from:

<http://arxiv.org/ps/astro-ph/0004259v1>

This figure "Fig3.png" is available in "png" format from:

<http://arxiv.org/ps/astro-ph/0004259v1>

This figure "Fig4.png" is available in "png" format from:

<http://arxiv.org/ps/astro-ph/0004259v1>

This figure "Fig5.png" is available in "png" format from:

<http://arxiv.org/ps/astro-ph/0004259v1>

This figure "Fig6.png" is available in "png" format from:

<http://arxiv.org/ps/astro-ph/0004259v1>

This figure "Fig7.png" is available in "png" format from:

<http://arxiv.org/ps/astro-ph/0004259v1>

This figure "Fig8.png" is available in "png" format from:

<http://arxiv.org/ps/astro-ph/0004259v1>

This figure "Fig9.png" is available in "png" format from:

<http://arxiv.org/ps/astro-ph/0004259v1>

This figure "Fig10.png" is available in "png" format from:

<http://arxiv.org/ps/astro-ph/0004259v1>

This figure "Fig11.png" is available in "png" format from:

<http://arxiv.org/ps/astro-ph/0004259v1>

This figure "Fig12.png" is available in "png" format from:

<http://arxiv.org/ps/astro-ph/0004259v1>

This figure "Fig13.png" is available in "png" format from:

<http://arxiv.org/ps/astro-ph/0004259v1>

This figure "Fig14.png" is available in "png" format from:

<http://arxiv.org/ps/astro-ph/0004259v1>

This figure "Fig15.png" is available in "png" format from:

<http://arxiv.org/ps/astro-ph/0004259v1>